

High-Speed Passenger Train Crashworthiness and Occupant Survivability

J. W. Simons and S. W. Kirkpatrick

SRI International, 333 Ravenswood Ave, Menlo Park, CA 94025

ABSTRACT - A calculational approach has been developed for crashworthiness analyses of train sets that is practical to perform using desktop workstations. The approach is organized into three steps. First, a detailed model of the train car is developed and the response of the car is calculated for various collision scenarios. Results of this first step highlight the response mechanism of the car and provide data on the crush strength of the car over a range of responses. The second step uses the crush response of the detailed model to develop simpler models that can be used to study the collision dynamics between cars. Using these simpler models allows calculation of the response of a set of several train cars in a collision or derailment scenario and includes interactions between cars. These calculations show how much crush each car experiences and provide velocity histories for different locations along the train set. The third step is to use the velocity histories for the cars to calculate the response of an occupant in the train. For this step, two procedures are described. First, a crash dummy and a few seats are modeled in detail and a simplified model is used for the surrounding car structure. Velocities are applied to the car structure and the secondary impact response of the occupant with the adjacent seats is calculated. Injury measures such as the head injury criterion (HIC) are obtained from the calculated acceleration records of the occupant head. The second procedure estimates injury by using relationships between secondary impact velocity, HIC, and injury. Examples of calculations for each of these steps are shown to illustrate this approach.

INTRODUCTION

As part of a program sponsored by The U.S. Federal Railroad Administration (FRA) and administered by the Volpe National Transportation Systems Center, a comprehensive risk assessment was performed of a generic high-speed U.S. train system to confirm a level of safety to passengers, crews, and the public that approaches or exceeds the level of safety achieved by existing and comparable modes of travel.

The objective of this program was to evaluate the accident survivability for a generic high-speed U.S. train system for various accident scenarios. The approach developed had three steps. The first step was to characterize the crushing response of individual cars. For this step, a detailed finite element model of a passenger car was developed from simplified assembly drawings. The crushing response of the car was determined by simulating a 26.8 m/s collision of the car with a 45 Mg rigid but moveable mass.

The second step was to characterize train collision dynamics. A simple finite element model of a passenger train car was developed that had crush characteristics similar to those calculated for the detailed car model. Several collision scenarios of a train set impacting either a rigid but moveable mass or a rigid wall were calculated. For each case, the number of seats lost in the cars was estimated based on the amount of car crush and the relative velocities were calculated for secondary impacts between the occupant and the train interior.

The third step was to calculate the occupant response. This was done in two ways. First, secondary impact calculations were performed using a fully deformable occupant model and a deformable seat model. As an injury measure, the head injury criterion (HIC) was calculated from occupant acceleration histories. This method was found to be very sensitive to details of the chair construction. The second method was to estimate injury using relationships between secondary impact velocity, HIC, and injury. The calculations for these tasks were performed using DYNA3D, a nonlinear, explicit, three-dimensional, finite element code [1].

CRASHWORTHINESS OF INDIVIDUAL CARS

A detailed model of a generic U.S. passenger car was developed from simplified assembly drawings. Figure 1 shows the car model with the outer skin and floor made invisible so that the

components of the superstructure and underframe are clearly visible. The model contains all the major and minor structural components, braces, as well as floor structures, wall structures, and the outer shell structure. Shell elements were used to build up geometrically accurate sections for the structural components. To account for the mass of the nonstructural components, a simplified interior configuration was included to increase the car mass to the correct value. The complete model of the car contains about 50,000 elements.

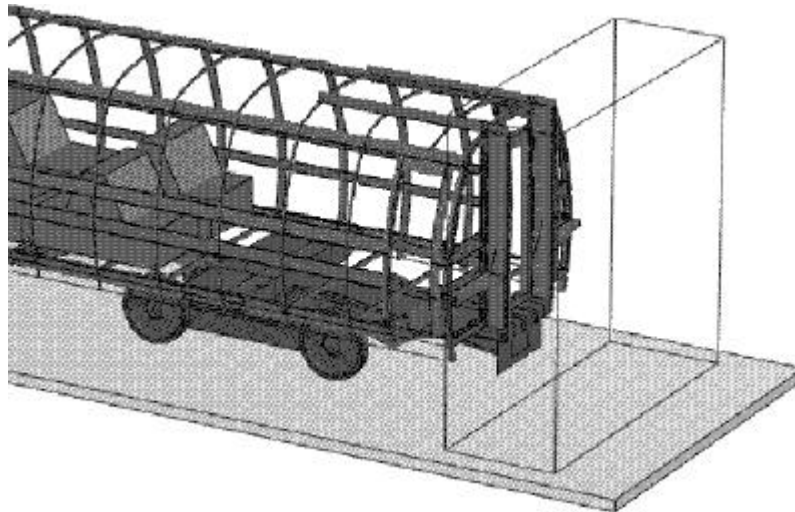


Figure 1. Detailed finite element model of generic U. S. passenger train car

Impact calculations and crush curves were calculated for a 26.8 m/s impact into a rigid but moveable 45 Mg mass (about equal to the mass of a train car). The mass was modeled with a smooth flat impact surface into which the car end impacted. Couplers and other equipment forward of the collision posts were not modeled. A rigid movable mass produces a collision response that is more severe than an impact with an equivalent crushable mass but is less severe than an impact into a rigid wall, because the mass can move.

Figure 2 shows the calculated crash response of the train car for the 26.8 m/s impact. The deformed shape of the car is shown at 0.050 s, which corresponds to a crush of approximately 1.0 m. The calculated deformations illustrate dynamic buckling of the outer skin.

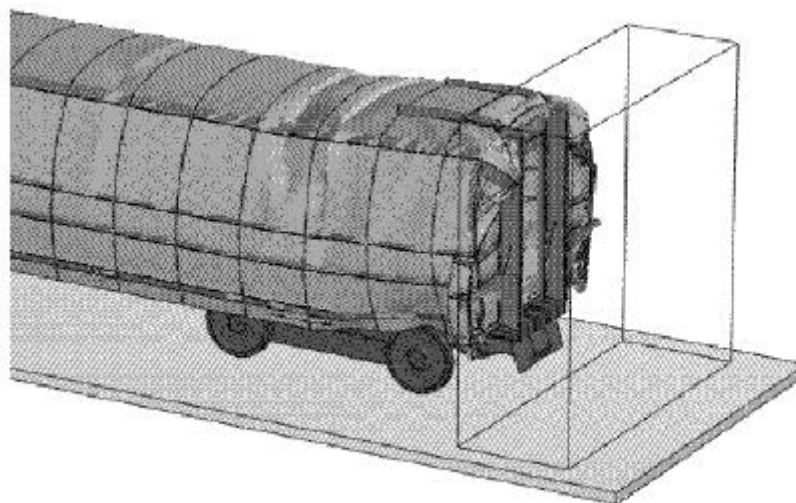


Figure 2. Calculated crash response for a 26.8 m/s impact with 45 Mg mass

Figure 3 shows the model with invisible skin and floor panels to illustrate the collapse mechanisms of the structural supports. The primary structural load path through the draft sill and center sill is compromised as the draft sill buckles dynamically upwards into the train compartment.

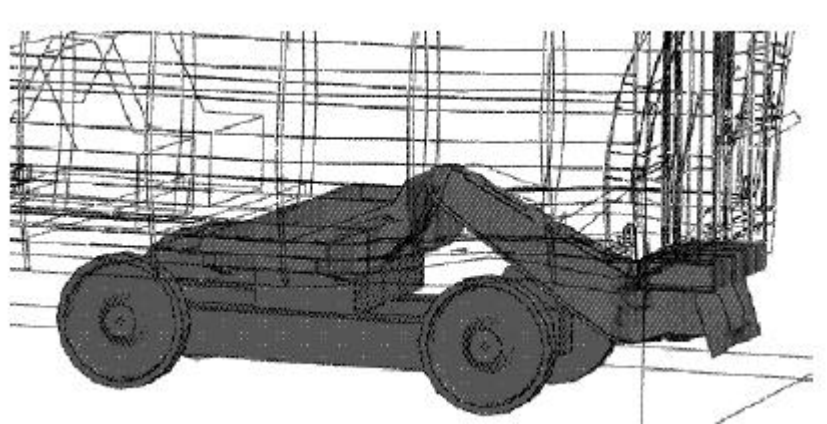


Figure 3. Calculated underframe crash response for a 26.8 m/s impact with 45 Mg mass

The calculated crush force and crash impulse as functions of time for the detailed model are shown in Figure 4. The peak force reached, about 27 MN, quickly drops to 9 MN, then levels off at a steady-state crushing force of about 2.5 MN. Steady-state crushing is reached at a time of approximately 20 ms, corresponding to a crush of approximately 0.5 m. The initial spike in force is primarily a dynamic effect, related to suddenly stopping the mass at the end of the car, and contributes significant impulse to the rigid mass. The impulse, found by integrating the force-time history of the train car, is equal to the total crash momentum imparted to the mass and corresponds to the change in velocity of the rigid mass.

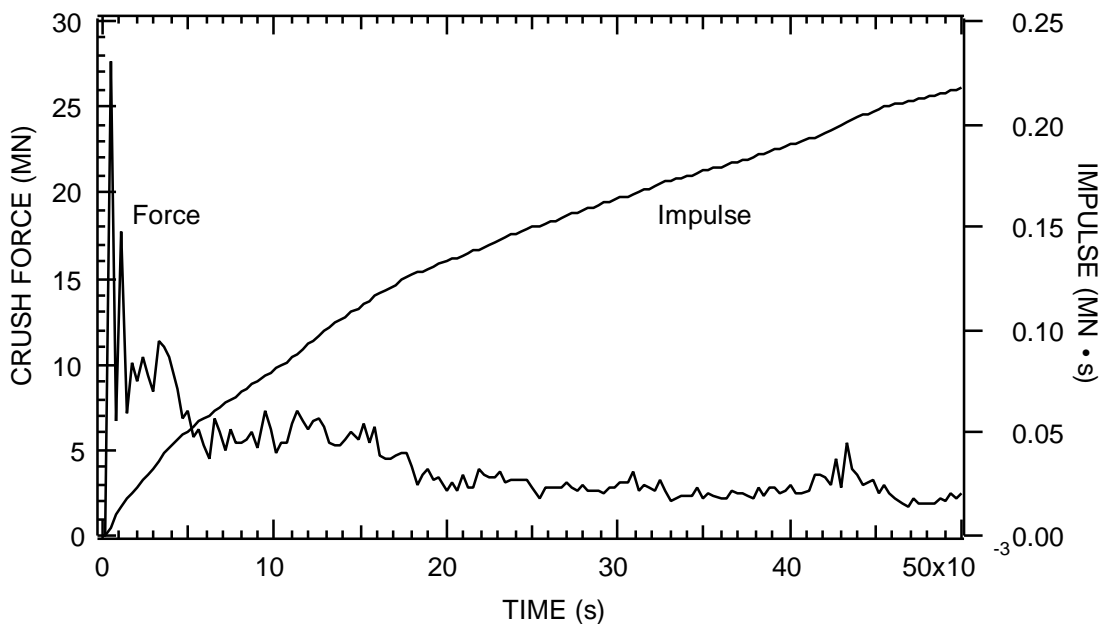


Figure 4. Calculated crush force and crash impulse 60 mph impact into a 50 ton mass

TRAIN COLLISION DYNAMICS AND STABILITY OF CONSISTS

To analyze the collision dynamics for the generic U. S. passenger train, a simplified crush model of a train car was developed using a solid crushable car with rigid bogies, as shown in Figure 5. A total of about 1500 elements were used for the car model.

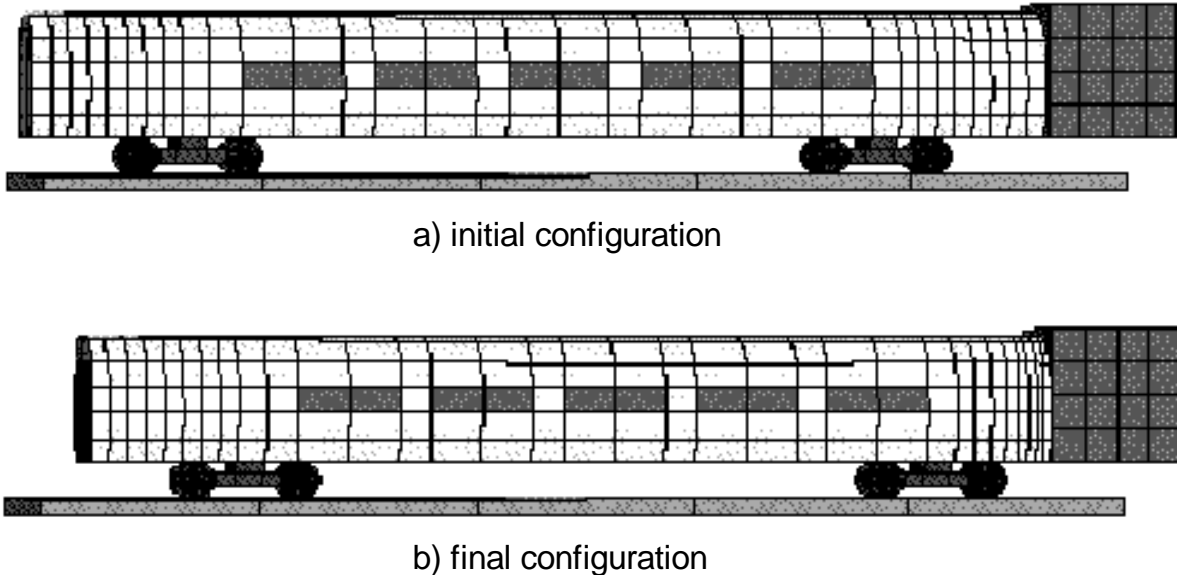


Figure 5. Finite element mesh for simple model of U.S. train car

The consist in our calculations had a power car followed by five coaches. The power car had a mass of 91 Mg, twice that of a passenger car [2]. The strength of the power car was twice that of a passenger car, consistent with assumptions described by Mayville et al. [3] in collision dynamics studies investigating locomotive crashworthiness. There was a 0.5 m gap between cars. The cars were restrained to one-dimensional motion.

The crush curve for the car material was assumed initially elastic with a modulus of 0.34 GPa and a constant crush strength of 0.34 MPa. At a true compressive strain of 1.3 (i.e., the material is 30% its original length), the material was assumed compacted with a modulus of 6.9 MPa. To validate the simple model, the 26.8 m/s detailed car collision with a 45 Mg mass was simulated. Figure 6 shows the resulting force-time and impulse-time curves for the detailed and simple model. The crush curve for the simple model reaches a peak force of about 27 MN followed by lower amplitude, damped oscillation to a steady-state crush force of about 3 MN. More important is the impulse curve, which corresponds directly to the change of velocity of the rigid mass and the train cars. The impulse for the simple model is slightly less than the detailed model initially, but the two curves intersect at a time of about 0.045 s.

Four collision scenarios with a rigid but moveable mass and three collision scenarios with a rigid wall were calculated. In US1-US4, the six-car consist impacts a rigid but moveable mass. The velocity of the train at the time of the collision is either 26.8 or 44.7 m/s and the mass is either 545 or 110 Mg. The parameters for these four cases are listed in Table 1. US5-US7 are collisions of the consist with velocities of 6.7, 13.4, and 22.4 m/s impacting a rigid wall. These scenarios correspond to symmetric head-on collisions with closing speeds of 13.4, 26.8, and 44.7 m/s respectively.

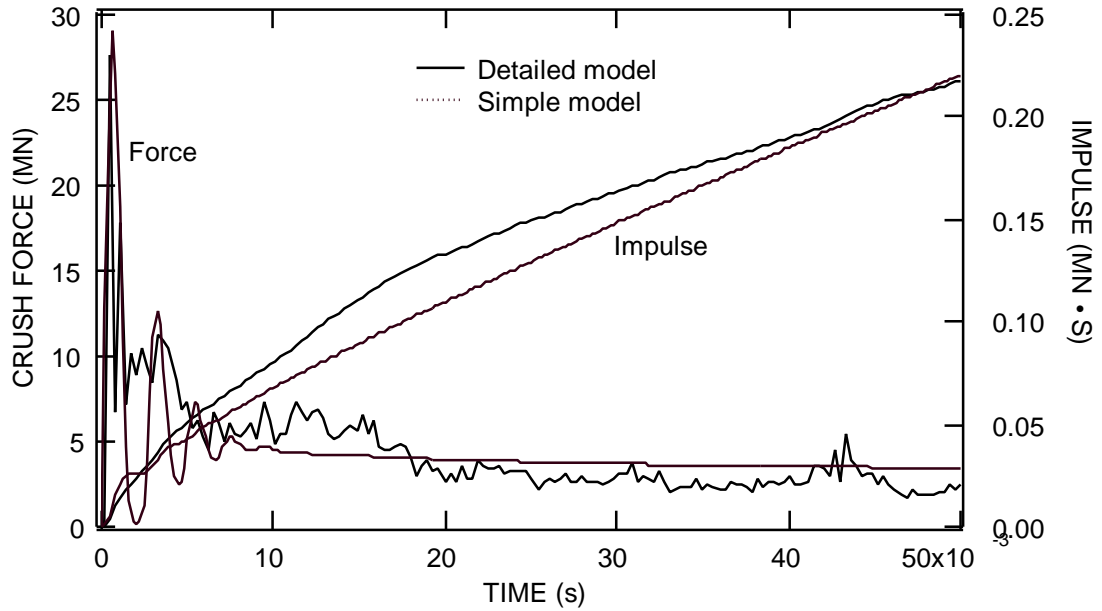


Figure 6. Calculated crush force and crash impulse for simple and detailed model

Table 1. Calculated car crush (meters) and seats lost* for the various collision scenarios

	US1 26.8 m/s 45 Mg	US2 26.8 m/s 110 Mg	US3 44.7 m/s 45 Mg	US4 44.7 m/s 110 Mg	US5 6.7 m/s Rigid Wall	US6 13.4 m/s Rigid Wall	US7 22.4 m/s Rigid Wall
Car 1 front	0.56 (0)*	1.70 (0)	1.40 (0)	6.10 (28)	0.46 (0)	4.10 (16)	10.2 (48)
Car 1 rear	0.15 (0)	0.51 (0)	0.46 (0)	1.60 (0)	0.20 (0)	1.02 (0)	5.59 (24)
Car 2 front	0.13 (0)	0.25 (0)	0.23 (0)	0.30 (0)	0.18 (0)	0.33 (0)	0.33 (0)
Car 2 rear	0.13 (0)	0.36 (0)	0.33 (0)	0.41 (0)	0.20 (0)	0.38 (0)	0.38 (0)
Car 3 front	0.10 (0)	0.18 (0)	0.15 (0)	0.23 (0)	0.13 (0)	0.25 (0)	0.25 (0)
Car 3 rear	0.08 (0)	0.30 (0)	0.28 (0)	0.33 (0)	0.20 (0)	0.33 (0)	0.33 (0)
Car 4 front	0.08 (0)	0.15 (0)	0.15 (0)	0.20 (0)	0.13 (0)	0.20 (0)	0.20 (0)
Car 4 rear	0.05 (0)	0.28 (0)	0.15 (0)	0.30 (0)	0.20 (0)	0.28 (0)	0.28 (0)
Car 5 front	0.05 (0)	0.13 (0)	0.13 (0)	0.13 (0)	0.10 (0)	0.13 (0)	0.13 (0)

- Values in parentheses represents the number of seats lost.

Figure 7 shows a representative calculated history for car velocities for scenario US4. The initial velocity of the consist is 44.7 m/s. The power car impacts the mass and starts to decelerate as the mass accelerates. At a time of about 0.3 s, the power car and mass reach the same velocity and move together from that time. The passenger cars decelerate one by one at intervals of about 0.1 s, with a nearly linear decrease in velocity corresponding to the nearly constant crush curve for the car. At a time of about 1.1 s, the consist and mass reach an equilibrium velocity of about 33.5 m/s which is consistent with a momentum balance for the collision.

Table 1 lists the calculated amount of crush in the cars for the seven scenarios. For each car, the amount of crush in the front and rear end was calculated by taking the final distance between the end of the car and the car center. In every case, the amount of crush is the greatest in the first car and decreases with each subsequent car.

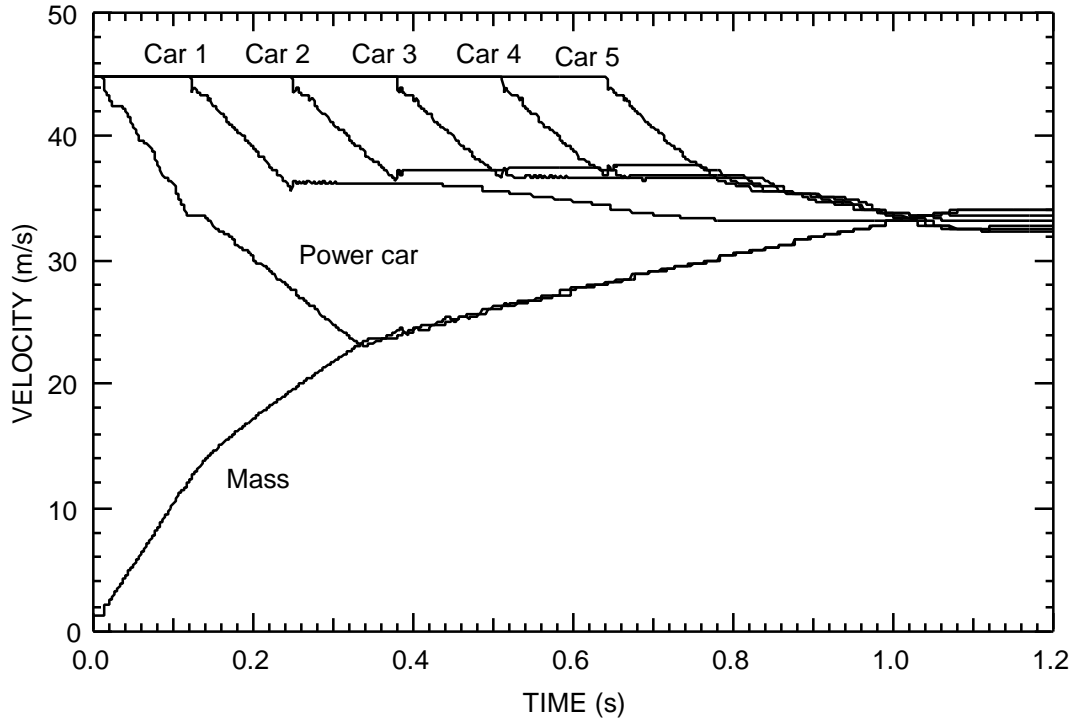


Figure 7. Velocity histories for collision scenario US4

For calculating seats lost due to crushing, an algorithm similar to that described by Tyrell et al. [4,5] was used. Assuming the volume of the crushed material occupies 30% of the original car length, the lost occupant volume can be calculated by dividing the reduction in length by 0.7. For example, the length of a completely crushed a car of length of 10 would be 3. The car crush, equal to the reduction in length would be 7, but the lost occupant volume would be 10 (e.g. $7/0.7$).

The lost occupant volume was translated into lost seats as follows. The car has about 2.9 m of unoccupied space at the end of the car with rest rooms, and 1.9 m of unoccupied space at the other end. Because the direction of the car is not known, the average of 9.0 m was assumed at each end. The total number of seats per car is 84 (21 rows of 4). No seats will be lost for the first 1.7 m of car crush and 4 seats will be lost for each additional 0.7 m of crush. All 4 seats were assumed lost once the crushed volume encroached a new row of seats. Using this algorithm, the front of Car 1 lost 28 seats for US4, 16 seats for US6, and 48 seats for US7 and the rear of Car 1 lost 24 seats for US7. No other seats were lost in any other collision scenario.

Sled testing of dummies shows the response of unrestrained occupants is decoupled from the response of the train car until the occupant strikes the forward seat back. As the car begins to decelerate from the primary collision, the occupant slides off the seat and continues to travel without significant velocity change. In the secondary collision, the occupant impacts the seat at a relative velocity depending on the car deceleration. Thus, the occupant does not feel the details of the acceleration pulse, only the change in velocity of the car during the time between the primary and the secondary collision.

Figure 8 shows the relative velocity as a function of relative displacement for collision scenario US4. There were no large differences in relative velocities for the different cars or different scenarios, even between those that produced very different amount of crush, because the decelerations are limited by the crush strength of the car. At a relative distance of about 0.5 m, the occupant's knees hit the forward seat back. Table 2 lists the relative velocities at impact for each of the seven collision scenarios.

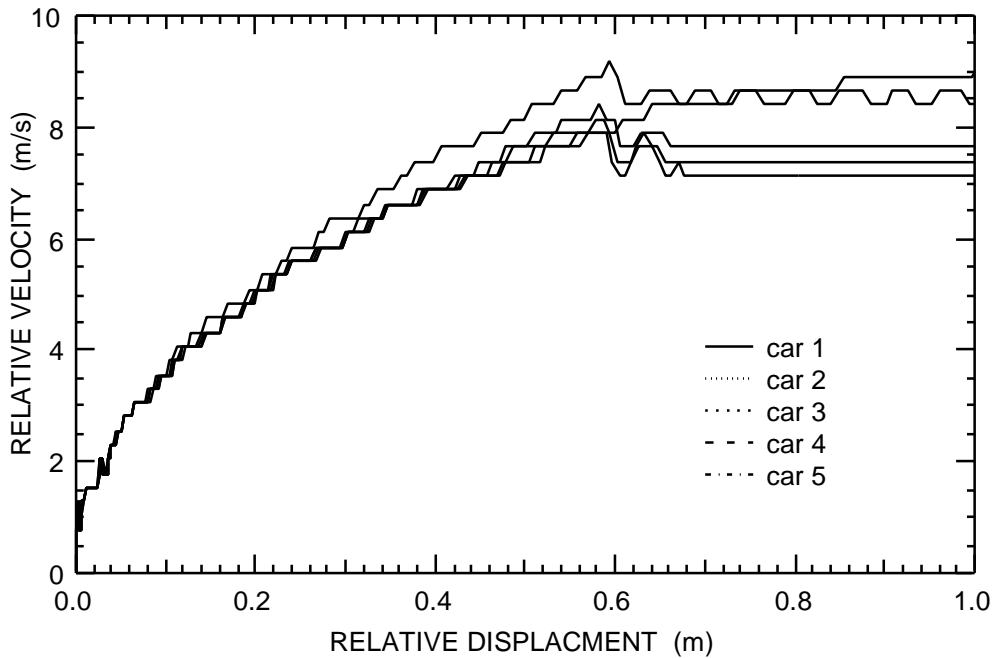


Figure 8. Relative velocity versus relative displacement for collision scenario US4

Table 2. Relative velocities for secondary collisions (m/s)

	US1	US2	US3	US4	US5	US6	US7
Car 1	7.61	8.06	6.27	8.06	7.61	8.51	8.51
Car 2	6.27	7.61	5.82	7.61	6.72	7.61	7.61
Car 3	5.82	7.61	5.82	7.61	7.17	7.61	7.61
Car 4	4.93	7.61	5.82	7.61	7.17	7.61	7.61
Car 5	4.03	7.61	5.82	7.61	7.17	7.61	7.61

For the calculations of collision dynamics, it was assumed that the cars remained in line. This assumption is probably unrealistic, especially for the higher speed collisions. In actual collisions, train consists commonly experience overall lateral buckling or override. However, sufficient information was not available on coupler characteristics or wheel-rail interaction to realistically model the couplings between cars and to investigate dynamic train stability.

INTERIOR ASSESSMENT

To assess injury risk from secondary collisions two methods were investigated. The first method was to perform detailed simulations of the occupant in the crash environment. The second method was to evaluate injury based relationships between interior stiffness, secondary impact velocity, and injury criteria.

Several detailed simulations were performed of secondary impact. The calculated responses showed a wide variability in the injury potential, depending on the specifics of the seat model. A representative calculation is shown in Figure 9. The interior model included two rows of double seats. The occupant impacts the seat back in the forward row. The seat was modeled with stiffness

characteristics estimated from static test data for the seat back high load application [6]. From dynamic test data [7], variations in the seat stiffness were considered to evaluate the effect of seat stiffness on injury potential. The occupant model was developed from SRI's SID model [8,9]. Several components (including arms and an abdominal insert) were added and joint flexibility was introduced in the hips, knees, and ankles.

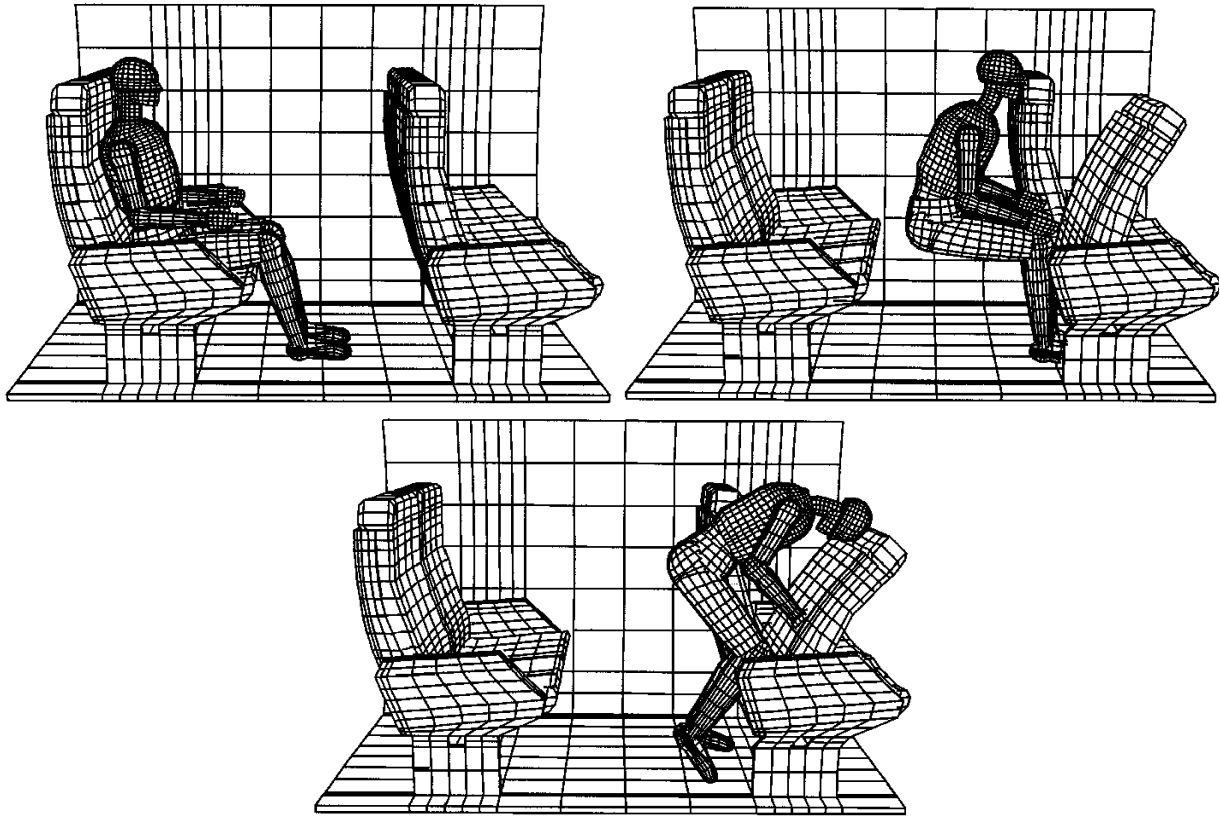


Figure 9. Calculated response for 6.7 m/s secondary collision

To simulate the secondary collision, the floor was given an acceleration history that produces the desired relative velocity at impact. Figure 9 shows the response of the occupant to a 6.7 m/s secondary impact. As the seat starts to decelerate, the occupant remains in much the same position. At a relative distance of about 0.5 m the occupant's knees hit the seat in front. The seats deform, and the occupant's head continues to move relatively forward. Because of the large forward rotation of the seat back, the occupant deforms considerably before his head impacts the seat. The collision of the occupant with the seat produces an upward rebound motion.

To relate head injury criterion (HIC) to injury, the procedure described by Tyrell et al [4-5] using the U.S. ISO delegation's recommended curve, shown in Figure 10, was used. For example, a collision that gives a HIC of 1000 gives a value a 18% for life-threatening injuries. There would be injuries among the remaining 82%, but not life-threatening injuries. The calculated value for HIC for the 6.7 m/s secondary collision was 101, corresponding to an injury level of zero. This value may be artificially low because the occupant still has a significant relative velocity compared to the car interior and is thrown over the top of the impacted seat.

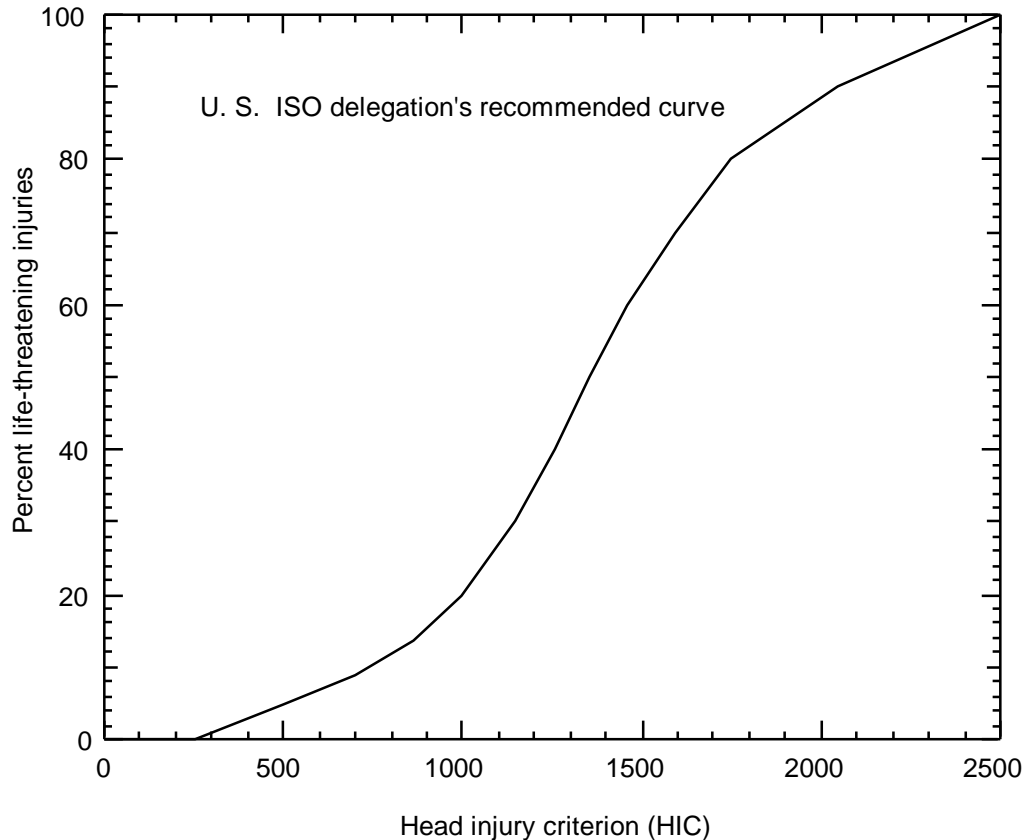


Figure 10. Percent life-threatening injuries as a function of HIC

Two calculations were performed for a secondary impact velocity of 9.0 m/s. The first used the same seat stiffness as in the 6.7 m/s simulation and the second used a stiffer value such that the plastic load limit of the seat back hinge equaled the peak load measured in the static load testing [6]. The calculated values of HIC were 77 for the soft seat back and 4,550 for the stiffer seat back. For the low stiffness seat, the seat back rotated forward and the occupant flew over the seat with little interaction. This behavior is seen in some dynamic sled tests in which the seats break away from their mounts resulting in very low HIC values. These calculations demonstrated the need for more accurate characterization of the dynamic response of the seat. Although good qualitative agreement of occupant kinematics and secondary collision response were obtained from these calculations, the wide variation in calculated HIC values made this method of interior assessment impractical.

Instead, to estimate the number of casualties from secondary collisions, a value of HIC was estimated based on the calculated relative velocity between the occupant and seat, and the procedure described above was used to relate HIC to casualties. To estimate HIC from relative velocity, we used results of simulations of head impact into bus seats. Figure 10 shows the results of HIC as a function of relative velocity for upper and lower bound seat stiffness. Table 3 lists values for HIC for the scenarios US1-US7 based on the relative velocities listed in Table 2. Two values are given corresponding to the lower and upper seat stiffness characteristics. The percentage of casualties corresponding to the value of HIC for each scenario is also listed in Table 3.

ACCIDENT SURVIVABILITY

Table 4 summarizes the overall accident survivability for the seven calculated collision scenarios. For each passenger car, the number of seats lost to crush was added to the number of casualties from secondary collisions assuming every seat is occupied. Casualties from crush and

Table 3. Range of HIC and percentage casualties* from secondary collisions

	US1	US2	US3	US4	US5	US6	US7
Car 1	199-806 (0-11.7%)	229-875 (0-14.3%)	199-806 (0-11.7%)	229-875 (0-14.3%)	199-806 (0-11.7%)	263-944 (0.2-17.4%)	263-944 (0.2-17.4%)
Car 2	122-619 (0-6.5%)	199-806 (0-11.7%)	102-564 (0-5.6%)	199-806 (0-11.7%)	145-678 (0-7.8%)	199-806 (0-11.7%)	199-806 (0-11.7%)
Car 3	102-564 (0-5.6%)	199-806 (0-11.7%)	102-564 (0-5.6%)	199-806 (0-11.7%)	171-741 (0-9.5%)	199-806 (0-11.7%)	199-806 (0-11.7%)
Car 4	67-456 (0-3.8%)	199-806 (0-11.7%)	102-564 (0-5.6%)	199-806 (0-11.7%)	171-741 (0-9.5%)	199-806 (0-11.7%)	199-806 (0-11.7%)
Car 5	41-360 (0-2.0%)	199-806 (0-11.7%)	102-564 (0-5.6%)	199-806 (0-11.7%)	171-741 (0-9.5%)	199-806 (0-11.7%)	199-806 (0-11.7%)

* Percentage casualties shown in parenthesis

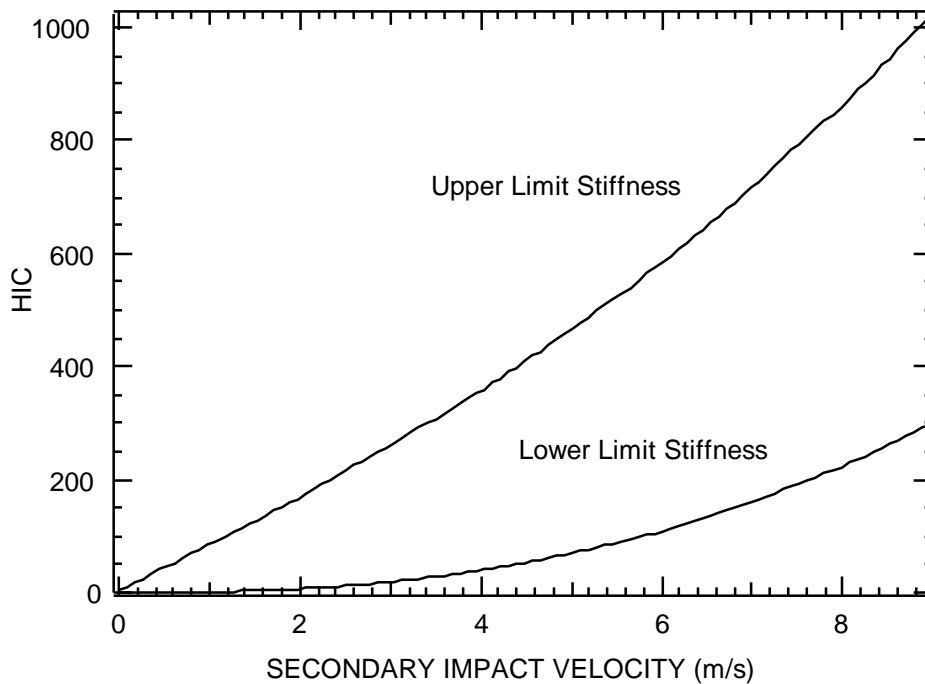


Figure 10. Head injury as a function of secondary impact velocity for crushable seats.

secondary collision are listed separately, with those due to crush shown in parentheses. The total number of casualties for all the cars is listed for each scenario. Casualties for the crew in the power car are not included, because the power car was not modeled with any fidelity. The lower bound for injuries may be artificially low because we have not considered passengers not seated in forward facing rows

who may have more potential for injuries, for example, passengers who are standing, or eating or in seats facing other passengers.

Table 4. Overall accident casualties*

	US1 60 mph 50 ton	US2 60 mph 120 ton	US3 100 mph 50 ton	US4 100 mph 120 ton	US5 15 mph Rigid Wall	US6 30 mph Rigid Wall	US7 50 mph Rigid Wall
Car 1	0-10	0-12	0-10	0-8 + (28)	0-10	0-8 + (16)	0-2 + (62)
Car 2	0-5	0-10	0-5	0-10	0-7	0-10	0-10
Car 3	0-5	0-10	0-5	0-10	0-8	0-10	0-10
Car 4	0-3	0-10	0-5	0-10	0-8	0-10	0-10
Car 5	0-2	0-10	0-5	0-10	0-8	0-10	0-10
Total (#)	0-25	0-52	0-30	28-76	0-41	16-64	62-104

* Range of casualties from secondary impact + seats lost to crushing (shown in parentheses).

REFERENCES

1. R. G. Whirley and J. O. Hallquist, "DYNA3D A Nonlinear, Explicit, Three-Dimensional Finite Element Code for Solid and Structural Mechanics - User Manual," University of California, Lawrence Livermore National Laboratory, UCRL-MA-107254, 1991.
2. M. R. Johnson, "Assessment of Crashworthiness of Locomotives," IITRI Final Report, Project VO6200 to Department of Transportation, Federal Railroad Administration, February 1993.
3. R. A. Mayville et al., "Locomotive Crashworthiness Research, Volume 1: Model Development and Validation," A. D. Little Inc., Final Report DOT-VNTSC-FRA-95-4.1 to U. S. DOT, Research and Special Projects Administration, Volpe National Transportation Systems Center, July 1995
4. D. C. Tyrell, K. J. Severson, and B. P. Marquis, "Train Crashworthiness Design for Occupant Survivability," presented at the Applied Mechanics Division of ASME Winter Annual Meeting, in San Francisco, California, November 12-17, 1995.
5. D. C. Tyrell, K. J. Severson, and B. P. Marquis, "Analysis of Occupant Protection Strategies in Train Collisions," presented at the Applied Mechanics Division of ASME Winter Annual Meeting in San Francisco, California, November 12-17, 1995.
6. Report for the Testing of Amtrak Traditional Seats to Rearward Loading Conditions for Collecting Baseline Data to Generate Future Safety Standards for Train Seats Dynamic Tests, MGA Research Corporation, MGA Ref. No. G95R-001, Prepared for VOLPE National Transportation Systems Center, August 1995.
7. Test Report, Department of Transportation Rail Passenger Seat Collision Performance: Traditional Seat Dynamic Tests, MGA Research Corporation, MGA Ref. No. G95R-001.2, Prepared for VOLPE National Transportation Systems Center, September 1995.
8. S. W. Kirkpatrick, B. S. Holmes, T. C. Hollowell, C. Gabler, and T. Trella, "Finite Element Modeling of the Side Impact Dummy (SID)," SAE Paper No. 930104 in *Human Surrogates: Design, Development, & Side Impact Protection*, SAE Publications, SP-945, pp. 75-86, Presented at the 1993 International Congress and Exposition, March 1993.
9. B. S. Holmes and S. W. Kirkpatrick, "Finite Element Model for Side Impact Dummy (SID)," Final Technical Report and Modeling Manual, PRC, Inc. Subcontract TSC-1, SRI Project PYU-3223, October 1992.